On Spectral Invariance of Single Scattering Albedo for Weakly Absorbing Wavelengths

Alexander Marshak[1], Yuri Knyazikhin[2], J. Christine Chiu[3], Warren J. Wiscombe[1]

[1]NASA Goddard Space Flight Center, code 613, Greenbelt, MD 20771, USA.
[2]Boston University, 675 Commonwealth Avenue, Boston, MA 02215, USA.
[3]Department of Meteorology, University of Reading, Reading, UK

Abstract

This note shows that for water droplets at weakly absorbing wavelengths, the ratio $\omega_{0\lambda}(r)/\omega_{0\lambda}(r_0)$ of two single scattering albedo spectra, $\omega_{0\lambda}(r)$ and $\omega_{0\lambda}(r_0)$, is a linear function of $\omega_{0\lambda}(r)$. The slope and intercept of the linear function are wavelength independent and sum to unity. This relationship allows for a representation of any single scattering albedo $\omega_{0\lambda}(r)$ via one known spectrum $\omega_{0\lambda}(r_0)$. The note provides a simple physical explanation of the discovered relationship. In addition to water droplets, similar linear relationships were found for the single scattering albedo of non-spherical ice crystals.

Keywords: single scattering albedo; droplets; ice particles; spectral invariance.

1. Introduction and the main result

The single scattering albedo in atmospheric radiative transfer is the ratio of the scattering coefficient to the total extinction coefficient (e.g., Bohren and Clothiaux, 2006, p. 257). It is equal to unity if all extinction is due to scattering (e.g., Rayleigh molecular scattering); conversely, it is equal to zero if all extinction is due to absorption (e.g., gaseous absorption). For spherical particles with a given refractive index single scattering albedo is calculated using Mie theory. For cloud water droplets both the scattering and absorption coefficients, thus the single scattering albedo, are functions of wavelength and droplet size. If the distribution of droplet sizes is given, both the coefficients and the single scattering albedo can be determined as functions of effective radius provided that the width of droplet size distribution is constant.

In general, the single scattering albedo ω_0, as a function of effective radius r and wavelength λ, is defined as,

$$\omega_{0\lambda}(r) = \frac{\sigma_{s\lambda}(r)}{\sigma_{s\lambda}(r) + \sigma_{a\lambda}(r)} \qquad (1)$$

where $\sigma_{s\lambda}$ and $\sigma_{a\lambda}$ are the scattering and absorption coefficients, respectively. To compute the single scattering albedo a Mie code (Bohren and Huffman, 1983) was run for four

wavelengths (0.86, 1.65, 2.13 and 3.75 μm) and for r from 5 to 50 μm (a gamma size distribution with effective variance 0.1 μm (Hansen and Travis, 1974) was assumed). When a ratio $\omega_{0\lambda}(r)/\omega_{0\lambda}(r_0)$ with r_0=5 μm was plotted against $\omega_{0\lambda}(r)$ as a function of the four wavelengths λ, a remarkable linear relationship was discovered:

$$\frac{\omega_{0\lambda}(r)}{\omega_{0\lambda}(r_0)} = p_1\omega_{0\lambda}(r) + p_2 \quad . \tag{2}$$

Here slope p_1 and intercept p_2 are wavelength independent parameters. Since $\omega_{0\lambda}(r)$=1 at λ=0.86 μm for all effective radii r, the sum of p_1 and p_2 is equal to 1, i.e. (2) can be rewritten as

$$\frac{\omega_{0\lambda}(r)}{\omega_{0\lambda}(r_0)} = p\omega_{0\lambda}(r) + (1-p) \quad . \tag{3}$$

Figure 1 illustrates Eq. (3) for r = 10, 20, 30 and 40 μm and r_0=5 μm. In the next section we provide a simple physical explanation of the spectral invariant relationship (3) and justify the results illustrated in Fig. 1.

2. Justification of the main results for water droplets

We start with the definition of the single scattering albedo (1). For the visible and near-infrared spectral regions, the scattering coefficient does not vary much with either wavelength or droplet size; we can assume it to be constant, i.e.,

$$\sigma_{s\lambda}(r) \equiv \sigma_s \quad . \tag{4}$$

Thus Eq. (1) can be rewritten as

$$\omega_{0\lambda}(r) = \frac{\sigma_s}{\sigma_s + \sigma_{a\lambda}(r)} \tag{5}$$

and the ratio of $\omega_{0\lambda}$ for two effective radii r and r_0 ($r_0 < r$) will be

$$\frac{\omega_{0\lambda}(r)}{\omega_{0\lambda}(r_0)} = \frac{\sigma_s + \sigma_{a\lambda}(r_0)}{\sigma_s + \sigma_{a\lambda}(r)} \quad . \tag{6}$$

Following Twomey and Bohren (1980), for weakly absorbing water droplets

$$1-\omega_{0\lambda}(r) \approx k_\lambda r \tag{7}$$

where k_λ is the bulk absorption coefficient (4π multiplied by the ratio of the imaginary part of the refractive index to wavelength). For wavelengths λ between 0.2 and 2.5 μm, the absorption coefficient $10^{-4}<k_\lambda<10^2$ cm^{-1} (Bohren and Clothiaux, Fig. 2.25, pg. 113).

Next, since

$$1-\omega_{0\lambda}(r)=\frac{\sigma_{a\lambda}(r)}{\sigma_s+\sigma_{a\lambda}(r)}, \tag{8}$$

it follows from Eq. (7) that

$$\frac{\sigma_s}{\sigma_{a\lambda}(r)}=\frac{\omega_{0\lambda}}{1-\omega_{0\lambda}}\approx\frac{1-k_\lambda r}{k_\lambda r} \tag{9}$$

and, neglecting the second order terms $o[(k_\lambda r)^2]$, we get

$$\sigma_{a\lambda}(r)\approx\sigma_s\frac{k_\lambda r}{1-k_\lambda r}=\sigma_s[k_\lambda r+(k_\lambda r)^2+(k_\lambda r)^3+\ldots]\approx\sigma_s k_\lambda r. \tag{10}$$

Let us now define a wavelength independent parameter p as

$$p = 1-r_0/r. \tag{11}$$

It follows that

$$r_0 = r(1-p). \tag{12}$$

We now rewrite the ratio (6) as

$$\frac{\omega_{0\lambda}(r)}{\omega_{0\lambda}(r_0)}=\frac{\sigma_s p+\sigma_s(1-p)+\sigma_{a\lambda}(r_0)}{\sigma_s+\sigma_{a\lambda}(r)}=p\omega_{0\lambda}(r)+\frac{\sigma_s(1-p)+\sigma_{a\lambda}(r_0)}{\sigma_s+\sigma_{a\lambda}(r)}. \tag{13}$$

Applying approximation (10) and relationship (12) to the second term in (13) gives

$$\frac{\sigma_s(1-p)+\sigma_{a\lambda}(r_0)}{\sigma_s+\sigma_s k_\lambda(r)}\approx\frac{\sigma_s(1-p)+\sigma_s k_\lambda r_0}{\sigma_s+\sigma_s k_\lambda r}=\frac{(1-p)+k_\lambda(1-p)r}{1+k_\lambda r}=1-p. \tag{14}$$

Equation (14) completes the "proof" of (3) with p defined by (11). Equation (3) is an approximation but it can be good enough for many purposes. Rearranging Eq. (3) leads to

$$\omega_{0\lambda}(r)=\omega_{0\lambda}(r_0)\frac{1-p}{1-p\omega_{0\lambda}(r_0)}. \tag{15}$$

Equation (15) states that the single scattering albedo $\omega_{0\lambda}(r)$ can be expressed via one known spectrum $\omega_{0\lambda}(r_0)$. Indeed, if one knows r and r_0, the slope $p=p(r,r_0)$ can be approximated by Eq. (11). However if r and r_0 are unknown, p can be obtained directly from Eq. (3). For example, if one knows the two single scattering albedos $\omega_{0\lambda}(r)$ and $\omega_{0\lambda}(r_0)$ at least at one weakly absorbing wavelength, say, λ=2.1 μm, then p can be determined from Eq. (3) as the slope between two points at λ=2.1 μm and at any visible wavelength since $\omega_{0\lambda}(r)=\omega_{0\lambda}(r_0)=1$ there. Knowing p, Eq. (15) provides $\omega_{0\lambda}(r)$ for any wavelength λ if $\omega_{0\lambda}(r_0)$ is available.

How well does Eq. (11) approximate the slope p as a function of r and r_0? Figure 2 illustrates two slopes: p from the Mie calculations and its approximation $p_{appr}=1-r/r_0$ as a function of r with given r_0=5 μm. In spite of a similar shape, there is a substantial difference which is due to approximation (7) and neglecting the second order terms $o[(k_\lambda r)^2]$ in (10). (In general, p is a linear function of the ratio r/r_0.) Left panel quantifies the difference between two slopes as a function of r.

3. Examples for ice crystals

Is Eq. (3) valid for non-spherical ice crystals? To check this we used the single scattering albedo for the Moderate Resolution Imaging Spectroradiometer (MODIS) ice phase function available at http://www.ssec.wisc.edu/~baum/Cirrus/MODIS_V2models.html (see Baum et al., 2005a and b) as well as for different types of ice crystals: bullet rosette, plates and hollow column provided by Dr. Ping Yang (see Yang et al., 2000). The results for the MODIS ice phase function are illustrated on Fig. 3. Though the correlation coefficients R are not as good as for the case of spheres illustrated in Fig. 1, the single scattering albedo for the ice crystals clearly shows the same spectral invariant behavior as the one described by Eq. (3). The slope p has a shape similar to Eq. (11), and can be well approximated by

$$p_{appr}(D) = 1-1.5D_0/D \qquad (16)$$

where D and D_0 are effective diameters. (We are not able yet to explain the factor 1.5 there.)

4. More Wavelengths

As mentioned earlier, Eq. (3) is valid for weakly absorbing wavelengths only. The weakly absorbing wavelengths are defined here as ones with bulk absorption coefficient $k_\lambda < 100$ cm^{-1} (thus for r=10 μm, $k_\lambda r < 0.1$ and $(k_\lambda r)^2 < 0.01$). Left panel in Fig. 4 illustrates the ratio between two single scattering albedo spectra $\omega_{0\lambda}(r)/\omega_{0\lambda}(r_0)$ for all wavelengths from 0.2 to 4 μm and droplet effective radii: r=20 μm, r_0=10 μm. In this plot wavelengths have been divided into two spectral regions: 0.2 to 2.5 μm (black dots) and 2.5 to 4 μm (grey dots). For the first region $k_\lambda < 100$ cm^{-1} while for the second one $k_\lambda > 100$ cm^{-1} (see the right panel in Fig. 4 adapted from Fig. 2.25 of Bohren and Clothiaux, 2006). The ratio for the weakly

absorbing spectral interval (0.2 – 2.5 μm) was fit with a linear function because contributions from the second order terms $o((k_\lambda r)^2)$ in (7) and (10) can be neglected there. The slope of the linear fit p=0.47 is close to the one (p=0.5) determined by Eq. (11) with r=20 μm and r_0=10 μm. We have also added the four wavelengths used in Fig. 1 (red dots). Note that λ=3.75 μm is just on the edge between the two spectral regions since $k_{3.75} \cong 100$ cm^{-1}.

5. Concluding Remarks

It was shown numerically and confirmed theoretically that the spectra of single scattering albedo $\omega_{0\lambda}(r)$ of water droplets of effective radus r at weakly absorbing wavelengths λ can be well approximated by another spectra $\omega_{0\lambda}(r_0)$ of effective radius r_0 using Eq. (15) assuming that the slope $p(r,r_0)$ between the ratio $\omega_{0\lambda}(r)/\omega_{0\lambda}(r_0)$ and $\omega_{0\lambda}(r)$ in the linear relationship (3) is known. The slope $p(r,r_0)$ can be approximated by a linear function of r/r_0 (see Eq. (11)). In addition to spherical water droplets, it was also shown using the MODIS ice phase function (Baum et al., 2005a) that the linear relationship (3) (and thus Eq. (15)) is valid for irregular ice crystals of different shapes (Yang et al., 2000). By weakly absorbing we mean all wavelengths with bulk absorption coefficient $k_\lambda < 100$ cm^{-1} (Bohren and Clothiaux, 2006, pg. 113).

We note that a spectral invariant relationship for single scattering albedo of green leaves was theoretically predicted by (Lewis and Disney, 2007). It was found that in the spectral interval between 710 nm and 790 nm, spectra of green leaves from different species (hazelnut, aspen, jack pine, etc.) were related to one fixed spectrum, called a reference spectrum, via Eq. (13); this property was used in classification of forest types from hyperspectral data (Schull et al., 2011).

Finally, linear relationship (3) and its counterpart (15) allow us to relate radiances as a function of single scattering albedo $\omega_{0\lambda}(r_0)$ to radiances at other single scattering albedos $\omega_{0\lambda}(r)$ in the spectrally invariant relationship between radiances discussed in Marshak et al. (2011). This study is yet in progress.

Acknowledgements
This research was supported by the Office of Science (BER, US Department of Energy, Interagency Agreement No. DE-AI02-08ER64562) as part of the ASR program. We also thank Drs. P. Gabriel, R. Kahn, A. Lyapustin, V. Martins, T. Varnai, Z. Zhang for fruitful discussions. We are grateful to Dr. P. Yang for providing a database which gives the phase function for individual ice crystals and Dr. Y. Yang for his help with Mie calculations.

REFERENCES

Baum, B.A., A. J. Heymsfield, P. Yang, S.T. Bedka, 2005: Bulk scattering properties for the remote sensing of ice clouds. Part I: Data and models. *J. Appl. Meteor.*, **44**, 1885–1895.

Baum, B.A., P. Yang, A.J. Heymsfield, S. Platnick, M.D. King, Y-X. Hu, S.T. Bedka, 2005: Bulk scattering properties for the remote sensing of ice clouds. Part II: Narrowband models. *J. Appl. Meteor.*, **44**, 1896–1911.

Bohren C. F. and D. R. Huffman, 1983: Absorption and Scattering of Light by Small Particles, 530 pp., J. Wiley & Sons, New York.

Bohren C. F. and D. R. Clothiaux, 2006: Fundamentals of Atmospheric radiation, 472 pp., J. Wiley-VCH Verlag GmbH & Co. KGaA, Weinheim.

Chiu, J. C., A. Marshak, Y. Knyazikhin, and W. J. Wiscombe, 2010: Spectrally-invariant behavior of zenith radiance around cloud edges simulated by radiative transfer. *Atmos. Chem. Phys.*, **10,** 11295-11303.

Hansen, J. E., and L. D. Travis, 1974: Light Scattering in Planetary Atmospheres, *Space Science Reviews,* **16**, 527–609.

Huang, D., Y. Knyazikhin, R. E. Dickinson, M. Rautiainen, P. Stenberg, M. Disney, P. Lewis, A. Cescatti, Y. H. Tian, W. Verhoef, J. V. Martonchik, and R. B. Myneni, 2007: Canopy spectral invariants for remote sensing and model applications. *Remote Sens. Environ.*, **106,** 106-122.

Knyazikhin, Y., J. V. Martonchik, R. B. Myneni, D. J. Diner, and S. W. Running, 1998: Synergistic algorithm for estimating vegetation canopy leaf area index and fraction of absorbed photosynthetically active radiation from MODIS and MISR data. *J. Geophys. Res.*, **103,** 32257-32275.

Knyazikhin, Y., M. A. Schull, L. Xu, R. B. Myneni, and A. Samanta, 2011: Canopy spectral invariants. Part 1: A new concept in remote sensing of vegetation. *J. Quant. Spectrosc. Radiat. Transfer*, **112,** 727-735.

Lewis, P. and M. Disney, 2007: Spectral invariants and scattering across multiple scales from within-leaf to canopy. *Remote Sens. Environ.*, **109,** 196-206.

Marshak, A., Y. Knyazikhin, J. C. Chiu, and W. J. Wiscombe, 2009: Spectral invariant behavior of zenith radiance around cloud edges observed by ARM SWS. *Geophys. Res. Lett.*, **36**, L16802, doi:10.1029/2009GL039366.

Marshak, A., Y. Knyazikhin, C. Chiu, and W. Wiscombe, 2011. Spectrally-invariant approximation within atmospheric radiative transfer. *J. Atmos. Sci.*, 68, 3094-3111.

Schull, M. A., Y. Knyazikhin, L. Xu, A. Samanta, P. L. Carmona, L. Lepine, J. P. Jenkins, S. Ganguly, and R. B. Myneni, 2011: Canopy spectral invariants, Part 2: Application to classification of forest types from hyperspectral data. *J. Quant. Spectrosc. Radiat. Transfer*, **112,** 736-750.

Twomey, S. and C. F. Bohren, 1980: Simple approximations for calculations of absorption in clouds. *J. Atmos. Sci.*, **37,** 2086-2094.

Yang, P., K. N. Liou, K. Wyser, and D. Mitchell, 2000: Parameterization of the scattering and absorption properties of individual ice crystals. *J. Geophys. Res.*, **105**, 4699–4718.

Figures

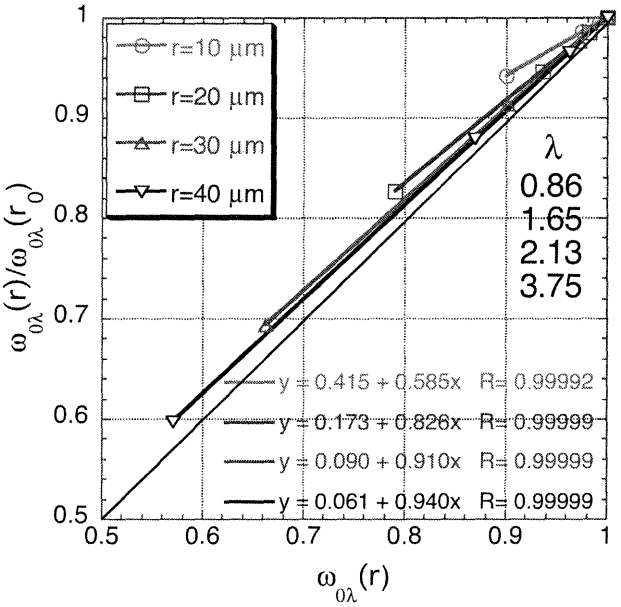

Figure 1. The ratio of $\omega_{0\lambda}(r)/\omega_{0\lambda}(r_0)$ plotted against $\omega_{0\lambda}(r)$ for four wavelengths λ=0.86, 1.65, 2.13 and 3.75. Single scattering albedos $\omega_{0\lambda}(r)$ are calculated using Mie theory. Droplet effective radius r=10, 20, 30, and 40 μm; r_0=5 μm. Droplet sizes are assumed to follow a gamma distribution with effective variance v =0.1 μm.

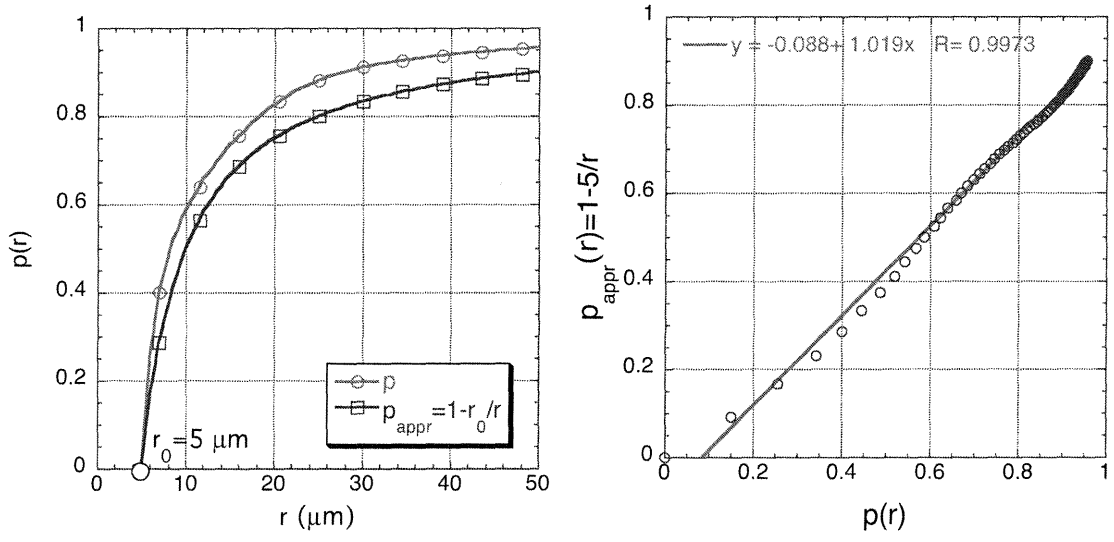

Figure 2. Two slopes p and p_{appr} as a function of r (**left panel**) and as a scatter plot (**right panel**). Slope p is from the Mie calculations using four wavelengths (0.86, 1.65, 2.13 and 3.75 μm) while slope p_{appr} is from Eq. (11) where r_0=5 μm.

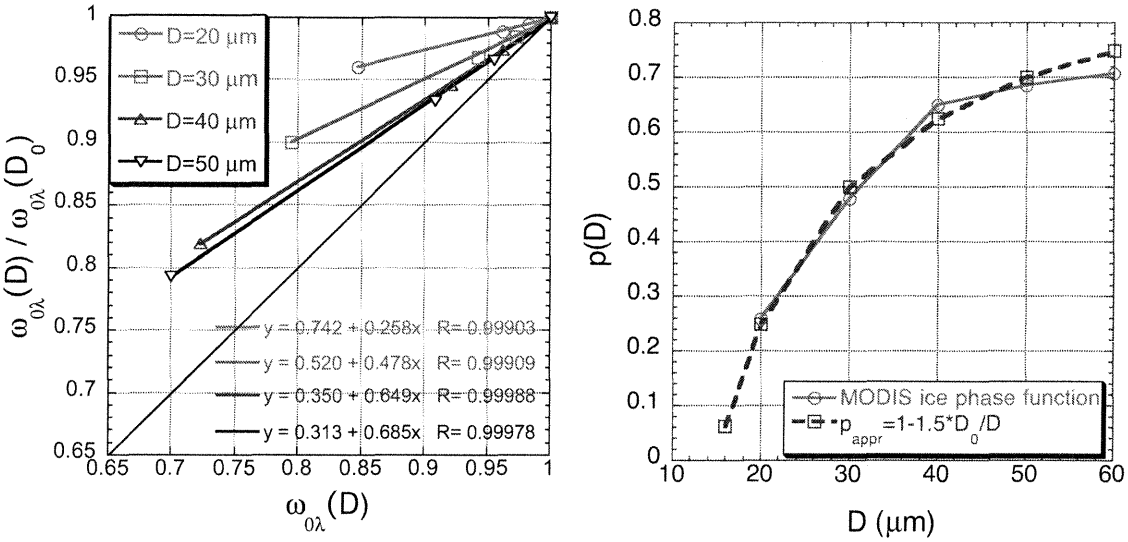

Figure 3. (**left**) The same as in Fig. 1 but for the MODIS ice phase function (Baum et al., 2005a) with effective diameter D_0=10 μm. (**right**) The same as in Fig. 2 (left panel) but for the MODIS ice phase function. The approximated slope is described by Eq. (16).

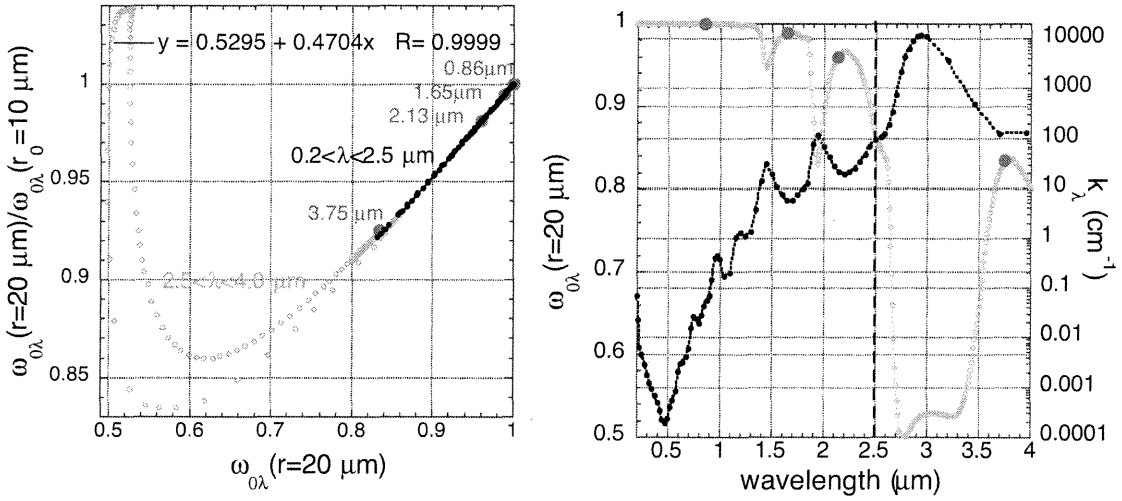

Figure 4. (**left**) The same as in Fig. 1 but for wavelengths λ between 0.2 μm and 4 μm with 10 nm spectral resolution; r=20 μm, r_0=10 μm. Grey open dots correspond to wavelengths between 2.5 and 4 μm while black filled dots to wavelengths between 0.2 and 2.5 μm. The linear fit is for the black dots only. Red dots correspond to the four wavelengths (0.86, 1.65, 2.13 and 3.75) used in Fig. 1. (**right**) The single scattering albedo $\omega_{0\lambda}(r)$ for r=20 μm and the bulk absorption coefficient as a function of wavelength. The bulk absorption coefficient, k_λ, was adapted from Fig. 2.25 of Bohren and Clothiaux (2006). The values of k_λ for liquid water were computed from the refractive index and wavelengths compiled by Querry et al. (1991). The red dots correspond to the same wavelengths as in left panel. The vertical dash line at 2.5 μm separates two spectral regions.